Available online at www.sciencedirect.com
ScienceDirect
Polymer 48 (2007) 1612–1619
polymer
www.elsevier.com/locate/polymer

Additives to improve the electret properties of isotactic polypropylene

Nils Mohmeyer [a,b], Nico Behrendt [c], Xiaoqing Zhang [d], Paul Smith [e], Volker Altstädt [c], Gerhard M. Sessler [d], Hans-Werner Schmidt [a,b,*]

[a] *Macromolecular Chemistry I, Bayreuther Institut für Makromolekülforschung (BIMF), University Bayreuth, D-95447 Bayreuth, Germany*
[b] *Bayreuther Zentrum für Grenzflächen und Kolloide (BZKG), University Bayreuth, D-95447 Bayreuth, Germany*
[c] *Polymer Engineering, University Bayreuth, D-95447 Bayreuth, Germany*
[d] *Institute for Communications Technology, Darmstadt University of Technology, D-64283 Darmstadt, Germany*
[e] *Department of Materials, Eidgenössische Technische Hochschule (ETH) Zürich, CH-8093 Zürich, Switzerland*

Received 11 April 2006; received in revised form 25 July 2006; accepted 3 August 2006
Available online 17 January 2007

Abstract

Substituted benzene-1,3,5-tricarboxylic acid trisamides are known to be efficient nucleating agents and in some selected cases are clarifiers for isotactic polypropylene (*i*-PP). In this paper we expanded the application range of this class of additives to the area of *i*-PP *electret* materials. This paper discusses in particular the relation between charge storage properties and additive concentration. Furthermore, attention is directed towards processing conditions, which were found to play an important role and seemed to be related to the dissolution and crystallization behavior of these additives from the *i*-PP melt. The formation of isolated nanometer-sized supramolecular structures was established to be important. It was found that, with the addition of benzene-1,3,5-tricarboxylic acid-(*N*-cyclohexyl)-trisamide, the charge storage properties of *i*-PP films can be improved at concentrations below 0.02 wt% (200 ppm). At such low concentrations, the additive appears to be present as isolated nano-aggregates, which can, therefore, efficiently act as charge traps. A further improvement in electret characteristics can be achieved by increasing the cooling rate of the polymer/additive blends. A clear correlation between nucleation efficiency and charge storage efficiency could not be revealed.

Keywords: Additives; Electret; Nanostructures

1. Introduction

Owing to excess charge on their surface, electret materials are used as self-adhesive films, microphone membranes, filter materials and in sensor technology to mention a few areas [1–7]. For these applications, mainly perfluorinated polymers such as polytetrafluoroethylene (PTFE), fluoroethylenepropylene (FEP) or polypropylene (PP) are employed, although they exhibit severe drawbacks in terms of processing and are substantially more expensive than polyolefins. Therefore, potential substitution of perfluorinated polymers by inexpensive and easy-to-process polymers has received increasing attention. In particular, the commodity polymer isotactic polypropylene (*i*-PP) has become of special interest as material for electrets, but until now, exhibits only moderate charge storage properties. Thus, modifications are needed to improve both the chargeability and the charge storage behavior of *i*-PP in order to approach the performance of fluorinated polymers [8,9].

There are two principal strategies that have been applied to improve the charge storage of polypropylene films. On the one hand, improvement of the charge stability can be achieved by introducing elongated voids during processing, resulting in porous films, however, at the expense of reduced transparency and mechanical properties [6,10–12]. On the other hand, the electret properties of polypropylene films can be improved by additives that function as charge traps [13] with little negative influence on optical and mechanical properties. In

* Corresponding author. Macromolecular Chemistry I, Bayreuther Institut für Makromolekülforschung (BIMF), University Bayreuth, D-95447 Bayreuth, Germany. Tel.: +49 921 55 3200; fax: +49 921 55 3206.
E-mail address: hans-werner.schmidt@uni-bayreuth.de (H.-W. Schmidt).

0032-3861/$ - see front matter © 2007 Elsevier Ltd. All rights reserved.
doi:10.1016/j.polymer.2006.08.001

a previous work, we reported a slight improvement in charge retention of about 10% for *i*-PP films containing certain triphenylamine-based trisamides [13]. Unfortunately, this class of compounds exhibits limited long-term light stability due to the oxidation of its triphenylamine core.

In the search for more stable and more efficient additives to improve the charge storage properties of *i*-PP, we investigated representatives of the class of benzene-1,3,5-trisamides, i.e. benzene-1,3,5-tricarboxylic acid-(*N*-cyclohexyl)-trisamide (**1**) and benzene-1,3,5-tricarboxylic acid-(*N-tert*-butyl)-trisamide (**2**) that were established to be efficient nucleating agents with excellent thermal and light stabilities, resulting in an additive concentration-dependent improvement of the optical properties (clarity and haze) [14–16] (Chart 1).

The aim of this paper is to present the general thermal, nucleation and optical properties of this class of compounds as additive in *i*-PP in correlation to their charge storage properties. We demonstrate the importance of the optimal additive content and how the performance as electret material can be improved by the processing conditions.

2. Experimental

2.1. Materials

Solvents used for synthesis were purified and dried according to standard procedures. Trimesic acid chloride and the amines were obtained from Aldrich and used as received. For all experiments, isotactic polypropylene reactor powder from Borealis (Linz, Austria), extracted with acetone, ethanol and cyclohexane, each for two days, was used. All other chemicals were used as received. ^{1}H NMR and ^{13}C NMR spectra were recorded at room temperature using a Bruker AC 250 instrument. IR spectra were recorded on a Bio-Rad Digilab FTS-40 (FT-IR) as KBr pellets. Mass spectra were obtained with a Mass Spectrometer Varian MAT CH-7 instrument (direct probe inlet, electron impact ionization).

2.2. Synthesis

2.2.1. General synthetic procedure for trisamides *1* and *2*

The amine compound (3.5 mmol) was dissolved in dry *N*-methyl-2-pyrrolidone (80 mL), dry triethylamine (10 mL), and approximately 0.05 g of dried LiCl were added. The trimesic acid chloride was added (1.0 mmol) and the mixture was stirred for 2 h at 80 °C. After cooling to room temperature, the mixture was precipitated in ice water (500 mL). The mixture was filtered (glass filter G3) to retrieve the solid, washed with water and dried. The resulting product was purified by recrystallization from DMF [16]. The ^{1}H NMR, ^{13}C NMR, IR, mass spectroscopy data and melting points (m.p.) of the individual compounds are given below.

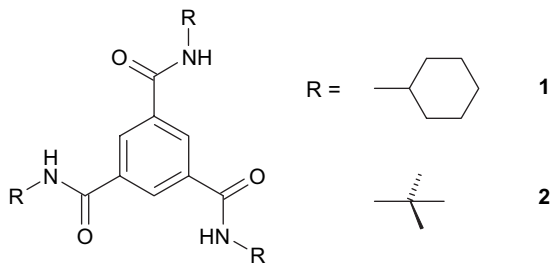

Chart 1. Chemical structures of the alkyl-substituted benzene-1,3,5-tricarboxylic acid trisamides (**1**–**2**), which act as nucleating agent and are used here to improve the electret properties of *i*-PP.

2.2.1.1. Benzene-1,3,5-tricarboxylic acid-(N-cyclohexyl)-trisamide (*1*)

Yield: 70%; m.p. 377 °C (under vapor.); ^{1}H NMR (DMSO-d_6, 250 MHz): $\delta = 1.01-2.05$ (m, 30H); 3.77 (m, 3H); 8.28 (s, 3H); 8.43 ppm (d, 3H); ^{13}C NMR ($CF_3COOD/CDCl_3$, 1:1): $\delta = 24.9$, 25.2, 32.2, 51.8, 130.7, 134.3, 168.0 ppm; IR (KBr, cm^{-1}): 3264 ν(NH), 3077 $\nu(CH_{arom.})$, 2932 $\nu(CH_{aliph.})$, 1650 ν(CO), 1542 $\nu(NH_{deform.})$; MS: *m/z* (%): 453 (46) [M$^+$].

2.2.1.2. Benzene-1,3,5-tricarboxylic acid-(N-tert-butyl)-trisamide (*2*)

Yield: 60%; m.p. sublimation 332 °C (no melting); ^{1}H NMR ($CF_3COOD/CDCl_3$, 1:1, 250 MHz): $\delta = 1.52$ (s, 27H); 8.51 ppm (s, 3H); ^{13}C NMR ($CF_3COOD/CDCl_3$, 1:1): $\delta = 27.9$, 55.1, 130.6, 135.0, 169.2 ppm; IR (KBr, cm^{-1}): 3231 ν(NH), 3067 $\nu(CH_{arom.})$, 2963, 2874 $\nu(CH_{aliph.})$, 1641 ν(CO), 1561 $\nu(NH_{deform.})$; MS: *m/z* (%): 375 (46) [M$^+$].

2.3. Methods

2.3.1. Film preparation

Polymer/additive mixtures were prepared in a laboratory-scale, co-rotating mini twin-screw extruder (Technical University Eindhoven, The Netherlands) at 240 °C under nitrogen for 4 min. The extruded mixtures were subsequently melted at 260 °C under nitrogen for 2 min and injection molded using a micro-injector (DACA Instruments, Goleta, CA), yielding circular specimens of 1.1 mm thickness and 25 mm diameter. Films of ~50 μm thickness were prepared by compression molding in a metal frame placed between Kapton® films and metal plates by melting at 260 °C for 3 min, subsequently pressing for 4 min at 15 kN in a laboratory press (P.O. Weber), followed by cooling to room temperature between the metal plates placed on a paper board resulting in an average cooling rate of about 10 K/min [calculated from 260 °C to 110 °C (*i*-PP crystallization)]. The cooling rate of 235 K/min was reached by placing the metal plates with the pressed film between two stainless steel plates at room temperature. To obtain the quenching effect with a cooling rate of 300 K/min, the two stainless steel plates were previously cooled in liquid nitrogen. These cooling rates were determined in separate experiments and calculated as average cooling rate between 260 °C and 110 °C.

2.3.2. Thermal properties

The melting temperatures and weight loss of the trisamides were determined by a coupled dynamic thermogravimetric

analysis (TGA) and differential thermal analysis (DTA) instrument, Netzsch STA 409. The crystallization temperature of *i*-PP/additive mixtures was determined by differential scanning calorimetry (DSC Diamond, Perkin Elmer). Measurements were performed with samples of 8–10 mg at a standard heating and cooling rate of 10 °C/min under nitrogen, starting from 130 °C to 230 °C. The samples were subsequently held at 230 °C for 5 min to ensure complete melting of the polymer, followed by cooling down to 50 °C. Reported values for the crystallization temperature (T_c) refer to the peak temperatures in the respective thermograms.

2.3.3. Optical properties

The standard optical characteristic "haze" was measured on injection-molded plaques (1.1 mm thickness) with a "Haze-Gard Plus" instrument (BYK Gardner GmbH, Germany) according to ASTM D-1003 [16].

2.3.4. Optical microscopy

For optical microscopy investigations, a granule of the respective extruded polymer/additive mixture was melted on a glass slide and protected with a cover glass. Micrographs were taken between crossed polarizers using a Nikon microscope equipped with a hot-stage (Mettler Toledo FP82HT) operated at a standard scan rate of 5 °C/min.

2.3.5. Transmission electron microscopy

The compression-molded *i*-PP films were embedded in an epoxy resin, EPO-TEK 301 (two components (hardener/gluten 1:3 v/v)), and cut with a microtome. The obtained 50–100 nm thick films were placed on a copper grid and stained for about 40 min with ruthenium tetraoxide. The grids were examined in a Zeiss CEM 902 electron microscope operating at 80 kV.

2.3.6. Charge storage properties

Films of 3×4 cm^2 area and about 50 μm thickness of the different polypropylene/additive mixtures were glued onto aluminium plates with conductive double-sided adhesive tape (Type: SPI-Supplies® brand carbon tape; thickness: 160 μm; conductivity: <5 ohm/square). All samples were charged for 60 s using a point-to-plate corona setup with a grid for limitation of the surface potential. A corona voltage of +12.5 kV and a grid voltage of +400 V were employed. The surface potential of each sample was measured with an electrostatic voltmeter (Monroe 244A). All reported data on surface potential values are the average of nine defined positions of the films. The reported data are average values for the nine spots with a deviation of less than ±10 V. Measurements were performed directly after charging at room temperature and after annealing at 90 °C for cumulative periods of 30, 90, 180, 360, 720 and 1440 min. The potential measurements were performed at room temperature outside the heating chamber. Thus, the samples were subjected to several heating and cooling cycles during the isothermal charge decay measurements [13].

3. Results and discussion

Since the two alkyl-substituted benzene-1,3,5-tricarboxylic acid trisamides selected for this study are similar in their thermal properties and nucleation behavior which are based on the same dissolution and self-assembly principle, the results will be discussed in the following predominantly with the cyclohexyl-substituted compound **1**, although the improvement of the electret performance is slightly different. Compound **1** was found to result in the best electret properties.

The trisamides were synthesized according to a general procedure starting from 1,3,5-tricarboxylic acid chloride, which was added at 80 °C to a solution of the amine in dry *N*-methyl-2-pyrrolidone (NMP), lithium chloride and triethylamine [16–18]. The benzene-1,3,5-tricarboxylic acid-(*N*-cyclohexyl)-trisamide (**1**) has a melting point at 376 °C and simultaneously vaporizes around this temperature, as was determined with a coupled dynamic thermogravimetric (TGA) and differential thermal analysis (DTA). This high melting point and the excellent thermal stability – generally found with this class of trisamides to be a substantial processing advantage – are caused by the amide linkages and the formation of well-ordered intermolecular hydrogen bonds. Like most other compounds of this family, at elevated temperatures compound **1** dissolves in small amounts in the *i*-PP melt and upon cooling from the melt, self-assembles into finely dispersed, one-dimensional, highly ordered fibrils, which provide a large surface capable of nucleating *i*-PP. These fibrils are tenuous three-dimensional superstructures, which – depending on concentration and processing parameters such as the cooling rate and presence of shear forces – may or may not become percolative in nature. Therefore, the concentration dependence of the solubility and self-assembly in the *i*-PP melt are expected to influence also the ability of certain members of this class of compounds to act as electret additives for *i*-PP.

The dissolution behavior of compound **1** in molten *i*-PP is presented as function of additive concentration in Fig. 1 (top). Dissolution temperatures were determined by polarized light microscopy as described elsewhere for a series of other benzene trisamides and sorbitol derivatives [14,15,19]. The dissolution temperatures were taken to be that temperature at which the last additive crystal disappeared completely in heating experiments in a polarized light microscope at a scan rate of 5 K/min. At concentrations below 0.02 wt% of compound **1** (regime *I*), no birefringent structures were detected in the *i*-PP melt, indicating that the supramolecular structures/crystals of the additive were either too small to be observed by polarized light microscopy or were completely dissolved. At concentrations between 0.02 wt% and 0.1 wt% (regime *II*), compound **1** was found to be completely soluble in the *i*-PP melt at the processing temperature of 260 °C (dashed line), whereas for higher concentrations (regime *III*), the additive remained partly insoluble. Fig. 1 (top) also shows the crystallization temperatures of *i*-PP/additive mixtures. The latter were determined by differential scanning calorimetry (DSC) as the peak temperatures of the exotherm in the thermograms that were recorded at a cooling rate of 10 K/min. As noted earlier and

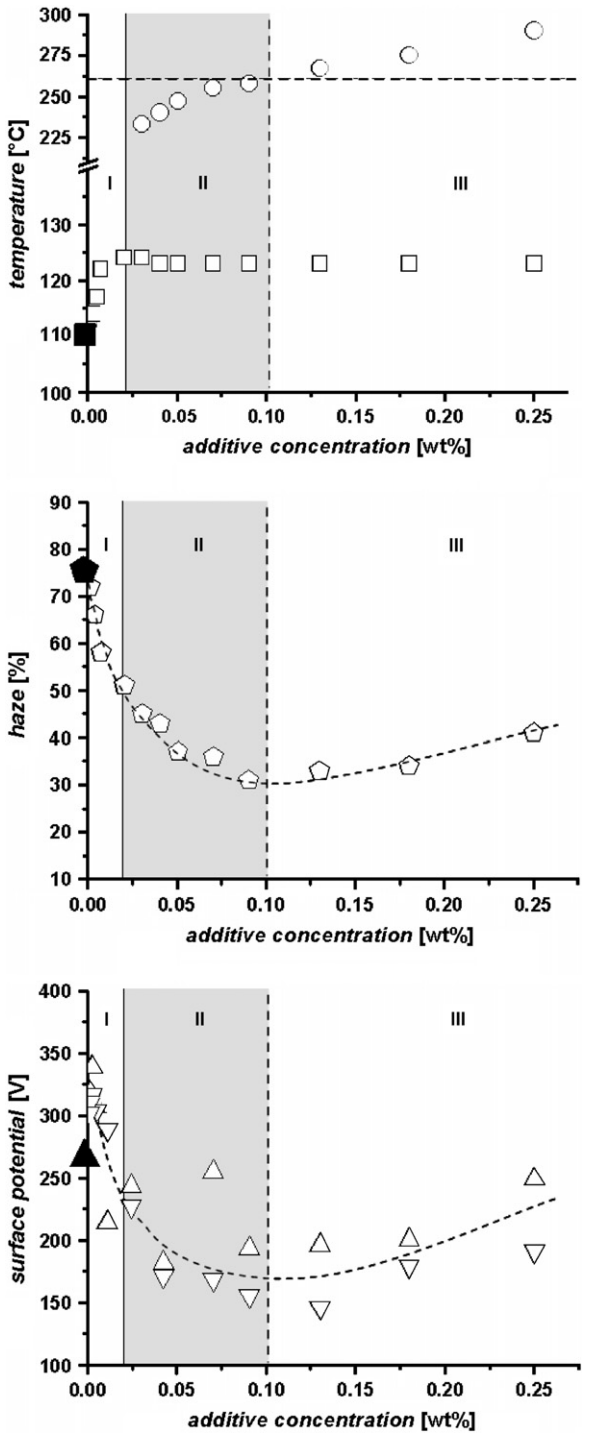

Fig. 1. Top graph: Additive dissolution temperature (○) and polymer crystallization temperature (□) for *i*-PP comprising compound **1**. The vertical dotted line at 0.1 wt% marks the concentration below which the additive is completely soluble in the *i*-PP melt at the employed processing temperature of 260 °C, indicated by the horizontal dashed line. Middle graph: Influence of the additive concentration on haze (open pentagon) of injection-molded *i*-PP plaques of 1.1 mm thickness. Bottom graph: Remaining surface potential of compression-molded *i*-PP films of 50 μm thickness, after annealing at 90 °C for 24 h, as function of the concentration of compound **1** for two independently prepared series (△, ▽). The films were prepared at a cooling rate of 10 K/min and initially charged with a corona voltage of +12.5 kV and a grid voltage of +400 V. In all graphs the reference values for neat *i*-PP are shown as closed symbols.

clearly can be seen, incorporation of compound **1** caused a substantial increase in the crystallization temperature from 110 °C of the neat *i*-PP (filled square) to 123 °C for additive concentrations exceeding 0.02 wt%. Below this concentration, an abrupt decrease in the crystallization temperature of *i*-PP was observed (regime *I*). To illustrate the above, Fig. 2A displays molten polypropylene comprising 0.04 wt% of compound **1** (regime *II*) at a temperature of 260 °C. At this concentration, the additive is completely dissolved as evidenced by the absence of any birefringent structures in the melt. Upon cooling, the additive crystallizes at around 240 °C. The formation of birefringent additive superstructures is shown in Fig. 2B, followed by crystallization of *i*-PP on the surface of the additive at a temperatures around 126 °C (Fig. 2C). By contrast, in concentration regime *III*, non-dissolved fibrillar structures of the additive are readily observed at 260 °C, as shown for a mixture comprising 0.25 wt% of compound **1** (Fig. 2D). Upon cooling of this mixture, the fibrillar network structure coarsened (Fig. 2E), presumably due to self-nucleation. Further cooling resulted in transcrystallization of *i*-PP onto the surface of the fibrils at 126 °C (Fig. 2F).

The solubility of the additive in molten *i*-PP also influences the optical properties of injection-molded plaques as previously described [14,15,19]. In Fig. 1 (middle), the additive concentration dependence of the haze values for 1.1 mm thick samples (open pentagon) is displayed. With increasing additive concentration, the haze value decreases from 74% for neat *i*-PP (filled pentagon) to a minimum of about 30% at around 0.1 wt% (regimes *I* and *II*), thereby improving the optical properties of the material. At higher concentrations (regime *III*), a fairly linear increase in haze was observed, which is attributed to the presence of undissolved additive particles that contribute to the scattering of the visible light.

The electret properties were determined as the surface potential of 50 μm thick compression-molded films (260 °C) prepared from the injection-molded specimen, which were used for the optical studies described above. The films were slowly cooled between the hot supporting metal plates, resulting in an average cooling rate of about 10 K/min. All samples were charged for 60 s by a point-to-plate corona setup with a grid for limitation of the surface potential. Corona voltages of +12.5 kV and grid voltages of +400 V were employed. The surface potential was measured under accelerated conditions at an elevated temperature of 90 °C over a period of 24 h. As mentioned in Section 2, the isotactic polypropylene powder was extracted with acetone, ethanol and cyclohexane to remove all processing aids and additives to obtain a neat base material.

In Fig. 3, the decay of the surface potential over time is shown for *i*-PP films comprising selected additive contents in comparison to the neat polypropylene reference. At very low additive concentrations (0.0024 wt% and 0.005 wt%) where the nucleation efficiency was low, if present at all (regime *I*), a remarkable improvement of the stability of the surface potential was observed. At a concentration of 0.0024 wt% (24 ppm), the highest value of the surface potential after 24 h annealing at 90 °C amounted to 339 V. This corresponds to relative charge retention of 87%, which is to be compared to

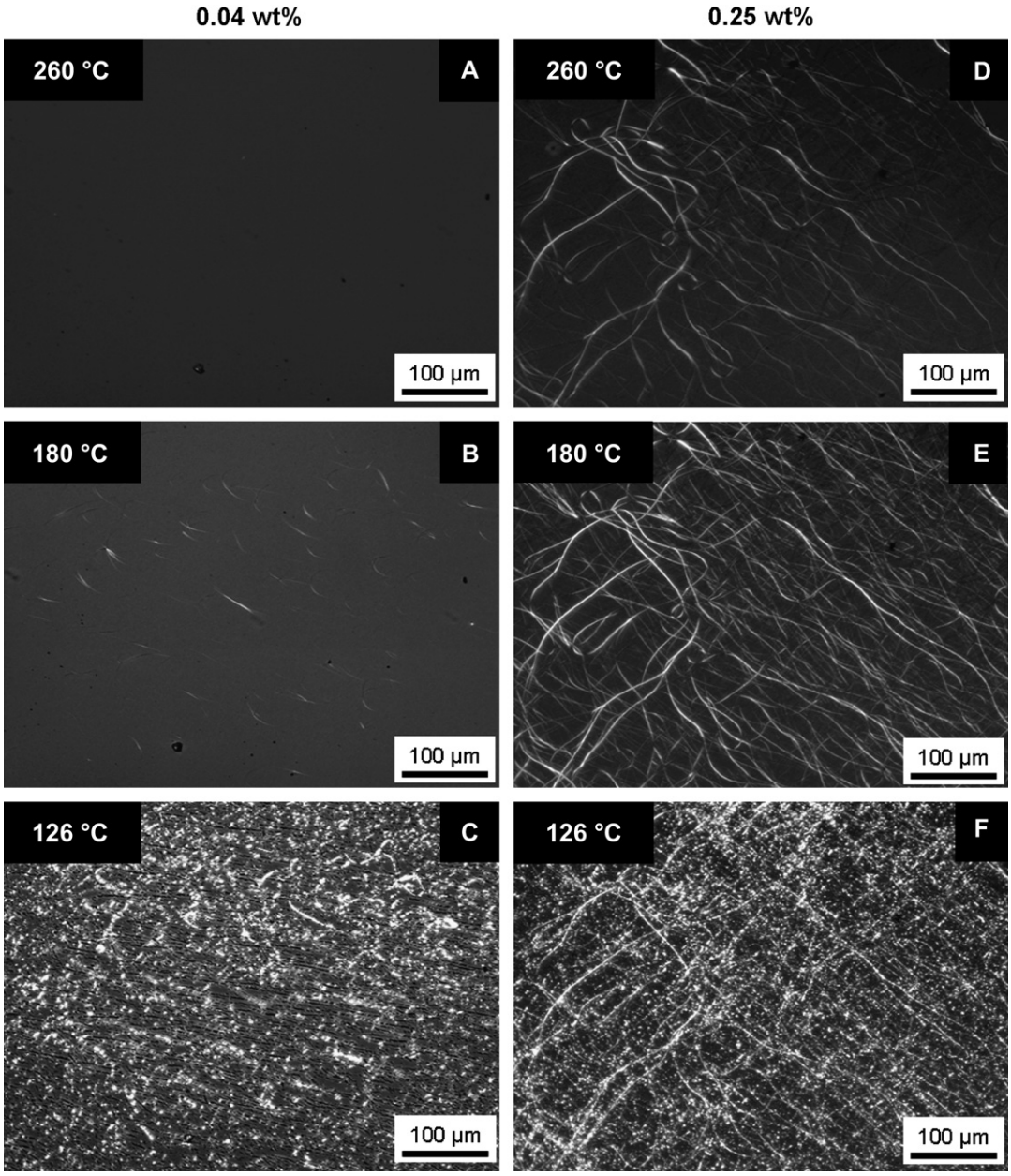

Fig. 2. Optical micrographs taken between crossed polarizers at various temperatures of *i*-PP samples comprising 0.04 wt% (left side) and 0.25 wt% (right side) of benzene-1,3,5-tricarboxylic acid-(*N*-cyclohexyl)-trisamide (**1**). At 126 °C (C, F), transcrystallization of *i*-PP onto the surface of the additive fibrils can be observed.

65% (260 V) for the reference material (filled triangle). Also included in Fig. 3 is the result obtained with a sample comprising 0.04 wt% of additive **1** (regime *II*), for which the surface potential of *i*-PP is clearly reduced.

The observed behavior of the remaining surface potential is probably due to two effects: at low additive concentrations (0.0024 wt%), the fluid-like structure of the neat polymer is changed to a semi-crystalline structure; this results in the generation of trapping centers at crystalline–amorphous interfaces or at other structural defects in the polymer. These localized states immobilize charges and thus result in a slower decrease of the surface potential. At larger concentrations (0.04 wt%), the additive introduces charge carriers in sufficient quantity into the polymer, thus causing a noticeable conductivity. This conductivity decreases the charge stability, as observed in the data in Fig. 3. The effects of these phenomena (trapping and conductivity) on the decay of the surface potential have been discussed in the literature, see summary in Ref. [1]. A comparison of two analytical approaches applicable to cases where carrier drift, carrier trapping, and conductivity are to be taken into account is given in Ref. [20]. In future work it is planned to apply an analytical treatment of this kind to the present data.

The trap structure of *i*-PP with and without additives is largely unknown. There have been many investigations with mostly indirect conclusions, based on X-ray, TSD and other studies or based on model calculations; see, e.g. Refs. [21,22]. Results of the latter study indicate that conformational traps in polymer insulating materials have relatively low

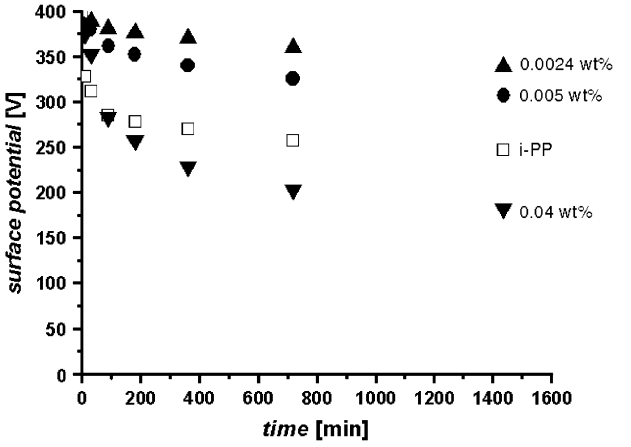

Fig. 3. Surface potential as function of annealing time at 90 °C of compression-molded *i*-PP films of 50 μm thickness containing different amounts of benzene-1,3,5-tricarboxylic acid-(*N*-cyclohexyl)-trisamide (**1**), in comparison with the *i*-PP reference (open squares).

activation energies (<0.3 eV) while traps caused by additives or impurities have larger depths up to and exceeding 1 eV. Increasing temperature is expected to cause an exponential increase of mobility if the mobility is trap controlled and therefore an accelerated potential decay. This decay changes also with time – particularly at long times. One relatively recent model takes the exhaustion of intrinsic conduction charges and the generation of new carrier pairs by environmental radiation into consideration [23]. The decay is initially almost exponential until the intrinsic charges are exhausted. Thereafter, the potential decay slows down and is governed by the generation of the new carriers.

The *tert*-butyl-substituted compound **2** exhibits a poorer solubility than compound **1** as well as a 30 °C higher dissolution temperature at a concentration of 0.02 wt%. The maximum surface potential in compound **2** was found at a concentration of 0.0002 wt% (about 10 times lower than that in compound **1**) with charge retention of 78%, and at a concentration of 0.0024 wt% (optimum of compound **1**) charge retention of 71% was determined. These results indicate that the phase behavior and the kinetics of the formation of isolated nanometer-sized structures are critical for the charge storage properties. The phase behavior and kinetics depend on the chemical structure of the additive and its solubility in the polymer matrix.

In order to illustrate the strong dependency of the surface potential on additive concentration in direct correlation to the solubility and optical properties, Fig. 1 (bottom) shows for two independently prepared series (△, ▽) the remaining surface potential after annealing at 90 °C for 24 h as function of additive concentration. For *i*-PP films, comprising less than 0.02 wt% of compound **1** (regime *I*), an improvement of the charge storage properties was observed. This regime *I* is characterized by low nucleation efficiency and no fibrillar structures were observed in the polymer melt, indicating the formation of isolated additive submicron-sized structures. In concentration regimes *II* and *III*, where a three-dimensional, percolating fibrillar network is observed, the charge storage properties are inferior to those of the reference material, indicating that the network provides pathways throughout the bulk of the sample, allowing the charge to drift and to be neutralized much faster. It is interesting to point out that the concentration dependence of both haze (Fig. 1, middle) and surface potential shows the same overall trend.

Transmission electron microscopy (TEM) studies were carried out to examine the nature of the additive structures in regime *I*, since their detection could not be accomplished by polarized optical light microscopy as mentioned above. Fig. 4 (top) shows the TEM image of an *i*-PP film comprising 0.01 wt% of compound **1** (regime *I*). Here, one of the isolated small additive crystals with a thickness of 20 nm is presented. With respect to the length of the additive aggregate no values

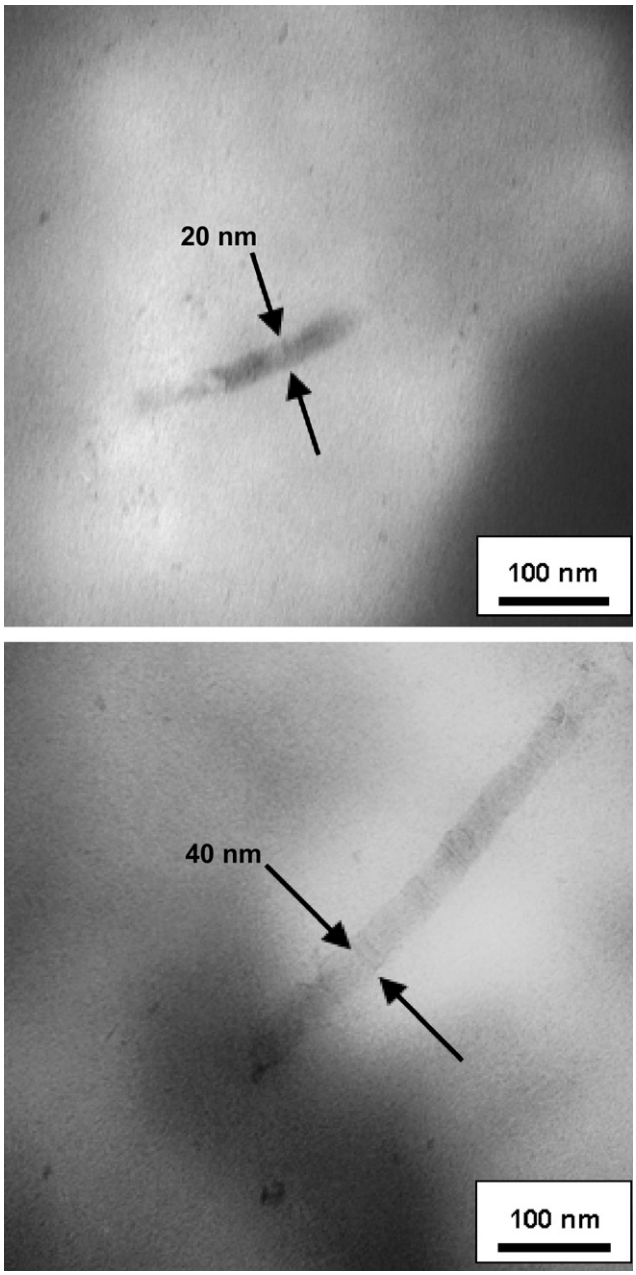

Fig. 4. Transmission electron microscopy pictures of slowly cooled (10 K/min) *i*-PP films comprising compound **1** at 0.01 wt% (top) (regime *I*) and 0.04 wt% (bottom) (regime *II*). The additive was stained with ruthenium tetraoxide.

can be given, as this depends on the position of the strong formanisotropic structure with respect to the cutting direction. At the higher concentration of 0.04 wt% of compound **1**, two-fold larger additive crystals with a thickness of about 40 nm were found.

Additional studies were conducted to examine the influence of the cooling rate, which is known to generally strongly affect nucleation densities and crystal sizes, on the decay of the surface potential.

In related work it was found that quenching of PP and FEP with cooling rates up to 120 K/min results in a slower potential decay and in increased temperatures of TSD peaks [24]. The effects were attributed to a reduction of the average crystallite size and to an increase in the number of crystal granules, resulting in an increase of the crystal/amorphous interface particularly in the surface regions of the samples where charge stability is best.

Therefore, we selected *i*-PP comprising 0.09 wt% of compound **1** (regime *II*), where the additive is completely soluble at 260 °C and shows a high nucleation efficiency with an *i*-PP crystallization temperature at 125 °C and causes a minimum haze value of 30%. At this concentration a three-dimensional fibrillar network structure is formed upon cooling at 10 K/min. In this case only a surface potential of 175–200 V can be retained, which is substantially below the *i*-PP reference (cooled at the same rate). The time dependence of the surface potential decay is shown in Fig. 5 (top) with a corresponding polarized

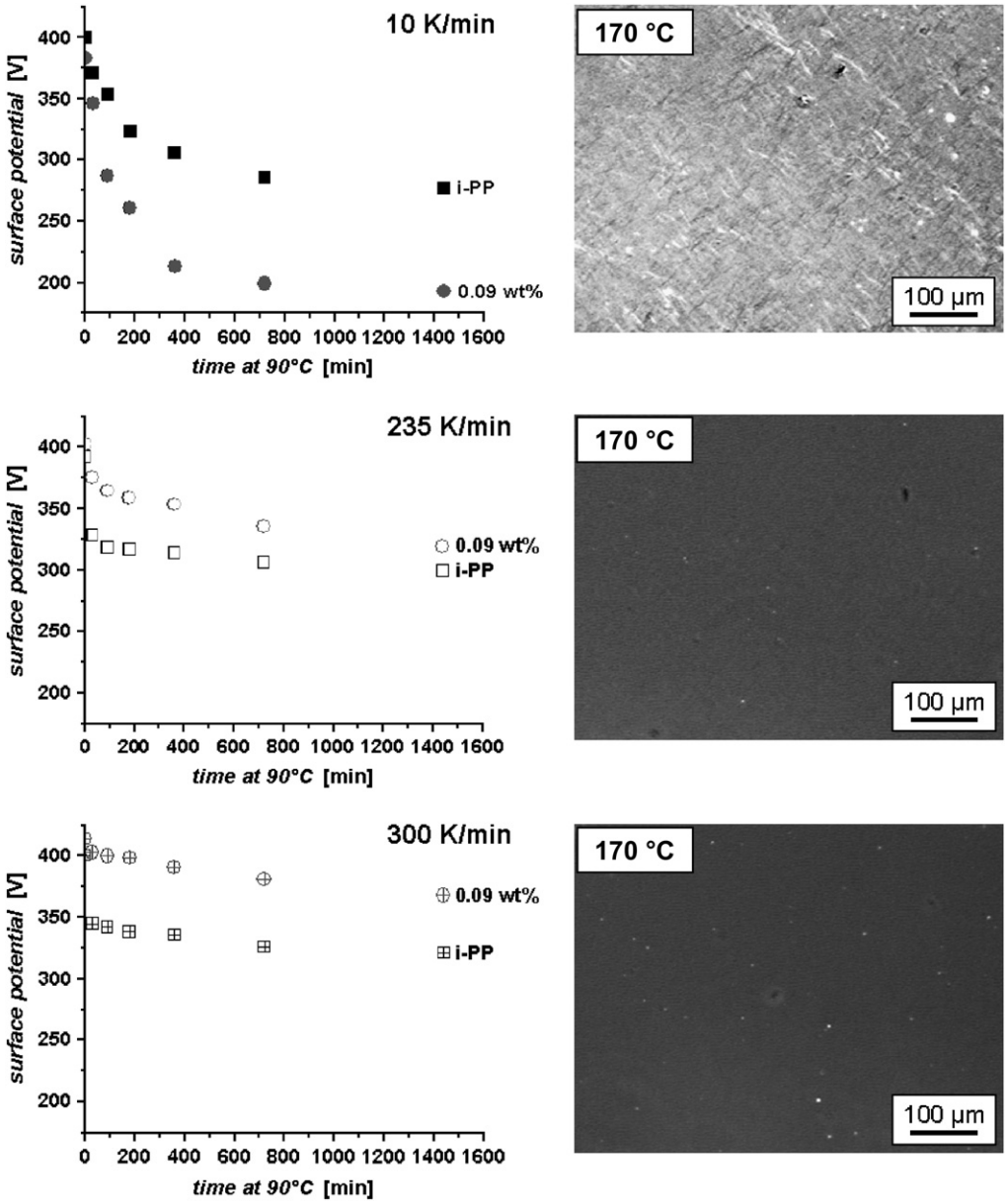

Fig. 5. Surface potential as function of annealing time at 90 °C of compression-molded *i*-PP films of 50 µm thickness with benzene-1,3,5-tricarboxylic acid-(*N*-cyclohexyl)-trisamide **1** at a concentration of 0.09 wt% (circle) in comparison with the *i*-PP reference treated under the same conditions (square). The films were produced at different cooling rates of 10 K/min (top), 235 K/min (middle) and 300 K/min (bottom). Corresponding polarized optical microscopy pictures were taken at 170 °C directly after melting the films.

optical light microscopy picture taken at 170 °C immediately after melting the sample. The picture clearly shows the pronounced birefringent network structure of the additive, which allows for the rapid discharge. To increase the cooling rate to 235 K/min, the film and the hot supporting metal plates were placed between two stainless steel plates at room temperature, reducing the time for a complete three-dimensional network formation of the additive. As is evident in Fig. 5 (middle), a strong stabilization of the surface potential was achieved. The surface potential values in the entire measurement time are higher than the corresponding values for the *i*-PP reference film, cooled at the same rate. Polarized optical microscopy shows no birefringent structures of the additive upon melting the film. A further improvement of the electret properties could be achieved by adopting a still higher cooling rate of 300 K/min (Fig. 5, bottom). This cooling rate was realized by placing the film and the hot supporting metal plates between two stainless steel plates, pre-cooled with liquid nitrogen. This resulted in a further improvement of the surface potential and an excellent charge storage behavior. The charge retention after 24 h at 90 °C was 89% and ~50 V higher than that found for the reference material cooled at the same conditions. Also here, as expected, polarized optical microscopy revealed no birefringent traces of the additive. In addition, the same experiments were carried out at much lower additive concentrations (0.0024 wt% and 0.005 wt%; regime *I*). In these experiments no improvement of the surface potential properties with increasing the cooling rate was observed. This can be explained by the fact that in regime *I*, isolated supramolecular aggregates are already formed at the employed relatively low cooling rate of 10 K/min.

By comparing the neat *i*-PP reference films prepared at the various cooling rates, increase in charge stability is observed. This observation is in agreement with the previous work of Ikezaki et al. on the improvement of the charge storage properties of polypropylene by reducing the polypropylene spherulite size [25].

4. Conclusions

In the present work we have demonstrated that certain nucleating agents based on substituted benzene-1,3,5-tricarboxylic acid trisamides are also efficient additives to improve the electret properties of isotactic polypropylene (*i*-PP). It was found that a strong correlation exists between the charge storage properties and the phase behavior of the additive, which depends on the chemical structure. In order to obtain excellent electret characteristics, the formation of a three-dimensional network structure of the additive, which acts as pathway for charge drift and neutralization, has to be prevented and isolated additive domains need to be generated to act as efficient charge traps. We found that, for this purpose, the additive concentration has to be decreased to a certain level – depending on the additive solubility and self-assembly process – to generate isolated additive domains. Further improvement of the charge storage behavior could be achieved by increasing the cooling rate applied during film processing. These results obtained with the selected compounds clearly demonstrate the potential of this class of additives to produce *i*-PP electret materials. In addition it should be mentioned that the nucleating and the charge storage efficiencies are not correlated.

Acknowledgment

We thank the Deutsche Forschungsgemeinschaft (DFG) for financial support (DFG-Projekte Schm 703/2-2; Al 474/5-2; Se 325/22-2). We are grateful to Dr. Joachim Hillenbrand (TU Darmstadt) for obtaining the experimental results shown in Figs. 1 (bottom one series), 3 and 4 and for stimulating comments on the manuscript. We thank Dr. Per Magnus Kristiansen (Ciba Specialty Chemicals, Basel, Switzerland) for helpful discussions on the broad class of trisamide nucleating agents. We are also indebted to Doris Hanft and Sandra Ganzleben (University Bayreuth) for their valuable assistance in the preparation of the additives and to Nicole Glaser (University Bayreuth) for performing transmission electron microscopy.

References

[1] Sessler GM. Electrets. New York: Springer Verlag; 1999.
[2] Nath R, Perlman MM. IEEE Trans Dielectr Electr Insul 1989;24:409–12.
[3] Gerhard-Mulhaupt R. Electrets. 3rd ed., vol. II. New York: Springer Verlag; 1999.
[4] Sessler GM, West JE. J Acoust Soc Am 1962;34:1787.
[5] Guarrotxena N, Millan J, Sessler GM, Hess G. Macromol Rapid Commun 2000;21:691.
[6] Mittal A, Jain V, Mittal JJ. Mater Sci Lett 2001;20:681–5.
[7] Myers DL, Arnold BD. Int Nonwov J 2003;12:43–54.
[8] Kressmann R, Sessler GM. IEEE Trans Dielectr Electr Insul 1996;3:607.
[9] Kawai H. Jpn J Appl Phys 1969;8:975.
[10] Hillenbrand J, Behrendt N, Altstädt V, Schmidt H-W, Sessler GM. J Phys D Appl Phys 2006;39:535–40.
[11] Nago S, Mizutani Y. J Appl Polym Sci 1998;68:1543–53.
[12] Behrendt N, Mohmeyer N, Hillenbrand J, Klaiber M, Zhang X, Sessler GM, et al. J Appl Polym Sci 2006;99:650–8.
[13] Mohmeyer N, Müller B, Behrendt N, Hillenbrand J, Klaiber M, Zhang X. Polymer 2004;45:6655–63.
[14] Blomenhofer M, Ganzleben S, Hanft D, Schmidt H-W, Kristiansen M, Smith P. Macromolecules 2005;38:3688–95.
[15] Kristiansen PM, Gress A, Smith P, Hanft D, Schmidt H-W. Polymer 2006;47:249–53.
[16] Blomenhofer M. Dissertation, University Bayreuth; 2003.
[17] Schmidt H-W, Smith P, Blomenhofer M. WO 02/46300 A2; 2002.
[18] Mäder D, Hoffmann K, Schmidt H-W. WO 03/102069 A1; 2003.
[19] Kristiansen M, Werner M, Tervoort T, Smith P, Blomenhofer M, Schmidt H-W. Macromolecules 2003;36:5150–6.
[20] Sessler GM, Figueiredo MT, Leal Ferreira GF. IEEE Trans Dielectr Electr Insul 2004;11:192–202.
[21] Ieda M, Suzuoki Y, Proc 5th Internat Conf on Propert and Applicat of Diel Mat; 1997. p. 16–23.
[22] Meunier M, Quirke N. J Chem Phys 2001;115:2876–81.
[23] Malecki JA. Phys Rev B 1999;59:9954–60.
[24] Xia Z. IEEE Trans Dielectr Electr Insul 1990;25:611–5.
[25] Ikezaki K., Fujii D. Proc – Int Symp Electrets, 7th 1991. p. 183–8.